

Energetics of the Microsporidian Polar Tube

Invasion Machinery

Supplementary Information

Ray Chang,[†] Ari Davydov,[‡] Pattana Jaroenlak,^{‡,¶} Breane Budaitis,[‡] Damian C. Ekiert,^{‡,§} Gira Bhabha,^{*,‡} and Manu Prakash^{*,†,||}

[†]*Department of Bioengineering, Stanford University, Stanford, California, United States of America*

[‡]*Department of Cell Biology, New York University School of Medicine, New York, New York, United States of America*

[¶]*Current Address: Center of Excellence for Molecular Biology and Genomics of Shrimp, Department of Biochemistry, Faculty of Science, Chulalongkorn University, Bangkok, Thailand*

[§]*Department of Microbiology, New York University School of Medicine, New York, New York, United States of America*

^{||}*Woods Institute for the Environment, Stanford University, Stanford, California, United States of America*

E-mail: gira.bhabha@gmail.com; manup@stanford.edu

Captions of supplementary videos

Supplementary Video S1: 3D reconstruction of ungerminated *A. algerae* spore from SBF-SEM data. Representative 3D reconstruction of an ungerminated *A. algerae* spore. At the beginning of the video, slices through the spore are shown. Each color represents an individual organelle: exospore (orange), endospore (yellow), PT (blue), posterior vacuole (red), and anchoring disc (green).

Supplementary Video S2: 3D reconstruction of an incompletely germinated *A. algerae* spore from SBF-SEM. Representative 3D reconstruction of an incompletely germinated *A. algerae* spore. At the beginning of the video, slices through the spore are shown. Each color represents an individual organelle: exospore (orange), endospore (yellow), PT (blue), posterior vacuole (red), nuclei (pink) and anchoring disc (green).

Supplementary Video S3: 3D reconstruction of a germinated *A. algerae* spore from SBF-SEM. Representative 3D reconstruction of a germinated *A. algerae* spore. At the beginning of the video, slices through the spore are shown. Each color represents an individual organelle: exospore (orange), endospore (yellow), PT (blue), and posterior vacuole (red). Note buckling of the spore body after cargo has been expelled.

Supplementary Video S4: Live-cell imaging of *A. algerae* PT germination in 0%MC.

Supplementary Video S5: Live-cell imaging of *A. algerae* PT germination in 4%MC.

Table S1: Selection of potential hypotheses.

J/E	OE	PTS	PTPV	PTC	ExP	abbreviation	reasons to exclude
J	X	X	X	X	X	-	isolated polar tube space.
J	O	X	X	X	X	-	cannot push the sporoplasm forward.
J	X	O	X	X	X	J-NOE-PTS*	-
J	X	X	O	X	X	-	only posterior vacuole is shot out.
J	X	X	X	O	X	-	cannot push the sporoplasm forward.
J	O	O	X	X	X	-	cannot generate pressure gradient.
J	O	X	O	X	X	-	only posterior vacuole is shot out.
J	O	X	X	O	X	-	OE and PTC are mutually exclusive.
J	X	O	O	X	X	-	PTS and PTPV are mutually exclusive.
J	X	O	X	O	X	-	PTS and PTC are mutually exclusive.
J	X	X	O	O	X	-	PTPV and PTC are mutually exclusive.
J	O	O	O	X	X	-	PTS and PTPV are mutually exclusive.
J	O	O	X	O	X	-	PTS and PTC are mutually exclusive.
J	O	X	O	O	X	-	PTPV and PTC are mutually exclusive.
J	X	O	O	O	X	-	PTS, PTPV and PTC are mutually exclusive.
J	O	O	O	O	X	-	PTS, PTPV and PTC are mutually exclusive.
J	X	X	X	X	O	-	isolated polar tube space.
J	O	X	X	X	O	-	cannot push the sporoplasm forward.
J	X	O	X	X	O	J-NOE-PTS-ExP	-
J	X	X	O	X	O	-	only posterior vacuole is shot out.
J	X	X	X	O	O	-	cannot push the sporoplasm forward.
J	O	O	X	X	O	-	cannot generate pressure gradient.
J	O	X	O	X	O	-	only posterior vacuole is shot out.
J	O	X	X	O	O	-	OE and PTC are mutually exclusive.
J	X	O	O	X	O	-	PTS and PTPV are mutually exclusive.
J	X	O	X	O	O	-	PTS and PTC are mutually exclusive.
J	X	X	O	O	O	-	PTPV and PTC are mutually exclusive.
J	O	O	O	X	O	-	PTS and PTPV are mutually exclusive.
J	O	O	X	O	O	-	PTS and PTC are mutually exclusive.
J	O	X	O	O	O	-	PTPV and PTC are mutually exclusive.
J	X	O	O	O	O	-	PTS, PTPV and PTC are mutually exclusive.
J	O	O	O	O	O	-	PTS, PTPV and PTC are mutually exclusive.
E	X	X	X	X	X	-	isolated polar tube space.
E	O	X	X	X	X	E-OE-PTN	-
E	X	O	X	X	X	-	everting content cannot go anywhere.
E	X	X	O	X	X	-	everting content cannot go anywhere.
E	X	X	X	O	X	E-NOE-PTC [†]	-
E	O	O	X	X	X	E-OE-PTS	-
E	O	X	O	X	X	E-OE-PTPV [‡]	-
E	O	X	X	O	X	-	OE and PTC are mutually exclusive.
E	X	O	O	X	X	-	PTS and PTPV are mutually exclusive.
E	X	O	X	O	X	-	PTS and PTC are mutually exclusive.
E	X	X	O	O	X	-	PTPV and PTC are mutually exclusive.
E	O	O	O	X	X	-	PTS and PTPV are mutually exclusive.
E	O	O	X	O	X	-	PTS and PTC are mutually exclusive.
E	O	X	O	O	X	-	PTPV and PTC are mutually exclusive.
E	X	O	O	O	X	-	PTS, PTPV and PTC are mutually exclusive.
E	O	O	O	O	X	-	PTS, PTPV and PTC are mutually exclusive.
E	X	X	X	X	O	-	isolated polar tube space.
E	O	X	X	X	O	E-OE-PTN-ExP	-
E	X	O	X	X	O	-	everting content cannot go anywhere.
E	X	X	O	X	O	-	everting content cannot go anywhere.
E	X	X	X	O	O	E-NOE-PTC-ExP	-
E	O	O	X	X	O	E-OE-PTS-ExP	-
E	O	X	O	X	O	E-OE-PTPV-ExP ^{††}	-
E	O	X	X	O	O	-	OE and PTC are mutually exclusive.
E	X	O	O	X	O	-	PTS and PTPV are mutually exclusive.
E	X	O	X	O	O	-	PTS and PTC are mutually exclusive.
E	X	X	O	O	O	-	PTPV and PTC are mutually exclusive.
E	O	O	O	X	O	-	PTS and PTPV are mutually exclusive.
E	O	O	X	O	O	-	PTS and PTC are mutually exclusive.
E	O	X	O	O	O	-	PTPV and PTC are mutually exclusive.
E	X	O	O	O	O	-	PTS, PTPV and PTC are mutually exclusive.
E	O	O	O	O	O	-	PTS, PTPV and PTC are mutually exclusive.

Table S1: Selection of potential hypotheses. (continued.)

J/E: jack-in-the-box ejection v.s. tube eversion.

OE: Original polar tube content open to the external environment post anchoring disc rupture.

PTS: Polar tube content is connected to sporoplasm.

PTPV: Polar tube content is connected to the posterior vacuole.

PTC: Polar tube is closed with solid content and cannot permit fluid flow.

ExP: Posterior vacuole expands during polar tube ejection.

*: Similar to the jack-in-the-box hypothesis.¹⁻³

†: Similar to the schematic drawing of Keeling & Fast 2002.⁴

‡: Similar to the hypothesis proposed by Findley 2005.⁵

††: Similar to the hypothesis proposed by Lom & Vavra 1963.⁶

Table S2: Summary of hypotheses.

J/E	OE	PTS	PTPV	PTC	ExP	abbreviation	topological compatibility	SBF-SEM evidence	energetics analysis
J	X	O	X	X	X	J-NOE-PTS*	compatible	incompatible	not analyzed
J	X	O	X	X	O	J-NOE-PTS-ExP	compatible	compatible	incompatible
E	O	X	X	X	X	E-OE-PTN	compatible	incompatible	not analyzed
E	X	X	X	O	X	E-NOE-PTC†	compatible	incompatible	not analyzed
E	O	O	X	X	X	E-OE-PTS	compatible	incompatible	not analyzed
E	O	X	O	X	X	E-OE-PTPV‡	compatible	incompatible	not analyzed
E	O	X	X	X	O	E-OE-PTN-ExP	compatible	compatible	compatible
E	X	X	X	O	O	E-NOE-PTC-ExP	compatible	compatible	likely compatible
E	O	O	X	X	O	E-OE-PTS-ExP	compatible	compatible	likely incompatible
E	O	X	O	X	O	E-OE-PTPV-ExP††	compatible	compatible	most compatible

J/E: jack-in-the-box ejection v.s. tube eversion.

OE: Original polar tube content open to the external environment post anchoring disc rupture.

PTS: Polar tube content is connected to sporoplasm.

PTPV: Polar tube content is connected to the posterior vacuole.

PTC: Polar tube is closed with solid content and cannot permit fluid flow.

ExP: Posterior vacuole expands during polar tube ejection.

*: Similar to the jack-in-the-box hypothesis.¹⁻³

†: Similar to the schematic drawing of Keeling & Fast 2002.⁴

‡: Similar to the hypothesis proposed by Findley 2005.⁵

††: Similar to the hypothesis proposed by Lom & Vavra 1963.⁶

Table S3: Methylcellulose does not change the germination rate of *A. algerae* spores. (p -value of logistic regression = 0.085.)

%MC	# germinated	total #	% germinated
0%	40	399	10.03%
0.5%	50	491	10.18%
1%	69	512	13.48%
2%	79	579	13.64%
3%	40	536	7.46%
4%	35	403	8.68%

Table S4: SBF-SEM observations on spore wall buckling.

Germinated spores	nucleus presence	no nucleus
buckling	1/25	21/25
no buckling	3/25	0/25
Incompletely germinated spores	nucleus presence	no nucleus
buckling	0/50	0/50
no buckling	50/50	0/50

Table S5: Sensitivity testing on cytoplasmic viscosity and boundary slip length (δ), considering the 2-fold length changes in PT before and after germination.

p -value [†] ($\delta = 0$ nm)	Model 1 J-NOE-PTS-ExP	Model 2 E-NOE-PTC-ExP	Model 3 E-OE-PTS-ExP	Model 4 E-OE-PTN-ExP	Model 5 E-OE-PTPV-ExP
$\mu_{\text{cyto}} =$ 0.001 Pa-sec	E: 9.9E-10* P: 4.2E-9* \dot{W} : 3.2E-9*	E: 0.389 P: 0.647 \dot{W} : 0.870	E: 0.197 P: 0.365 \dot{W} : 0.277	E: 0.298 P: 0.688 \dot{W} : 0.808	E: 0.402 P: 0.463 \dot{W} : 0.902
$\mu_{\text{cyto}} =$ 0.05 Pa-sec	E: 1.7E-6* P: 0.013* \dot{W} : 4.8E-5*	E: 0.194 P: 0.828 \dot{W} : 0.852	E: 0.054* P: 0.057* \dot{W} : 0.123	E: 0.134 P: 0.584 \dot{W} : 0.632	E: 0.331 P: 0.477 \dot{W} : 0.918
$\mu_{\text{cyto}} =$ 0.8 Pa-sec	E: 0.200 P: 0.807 \dot{W} : 0.330	E: 0.190 P: 0.832 \dot{W} : 0.852	E: 0.050* P: 0.055* \dot{W} : 0.120	E: 0.134 P: 0.570 \dot{W} : 0.632	E: 0.323 P: 0.476 \dot{W} : 0.918
$\mu_{\text{cyto}} =$ 10 Pa-sec	E: 0.048* P: 0.781 \dot{W} : 0.157	E: 0.190 P: 0.832 \dot{W} : 0.852	E: 0.050* P: 0.055* \dot{W} : 0.120	E: 0.134 P: 0.570 \dot{W} : 0.632	E: 0.323 P: 0.476 \dot{W} : 0.918
p -value ($\delta = 15$ nm)	Model 1 J-NOE-PTS-ExP	Model 2 E-NOE-PTC-ExP	Model 3 E-OE-PTS-ExP	Model 4 E-OE-PTN-ExP	Model 5 E-OE-PTPV-ExP
$\mu_{\text{cyto}} =$ 0.001 Pa-sec	E: 7.5E-10* P: 1.6E-9* \dot{W} : 1.7E-9*	E: 4.6E-4* P: 0.013* \dot{W} : 0.029*	E: 1.6E-7* P: 4.4E-5* \dot{W} : 6.1E-6*	E: 0.017* P: 0.052* \dot{W} : 0.106	E: 0.048* P: 0.085 \dot{W} : 0.170
$\mu_{\text{cyto}} =$ 0.05 Pa-sec	E: 1.5E-8* P: 4.1E-5* \dot{W} : 1.4E-7*	E: 0.378 P: 0.440 \dot{W} : 0.794	E: 0.086 P: 0.123 \dot{W} : 0.177	E: 0.235 P: 0.836 \dot{W} : 0.925	E: 0.303 P: 0.469 \dot{W} : 0.920
$\mu_{\text{cyto}} =$ 0.8 Pa-sec	E: 0.0076* P: 0.776 \dot{W} : 0.109	E: 0.327 P: 0.431 \dot{W} : 0.784	E: 0.031* P: 0.082 \dot{W} : 0.120	E: 0.213 P: 0.849 \dot{W} : 0.926	E: 0.291 P: 0.476 \dot{W} : 0.915
$\mu_{\text{cyto}} =$ 10 Pa-sec	E: 0.089 P: 0.771 \dot{W} : 0.204	E: 0.327 P: 0.431 \dot{W} : 0.784	E: 0.028* P: 0.082 \dot{W} : 0.120	E: 0.213 P: 0.843 \dot{W} : 0.926	E: 0.284 P: 0.476 \dot{W} : 0.915
p -value ($\delta = 60$ nm)	Model 1 J-NOE-PTS-ExP	Model 2 E-NOE-PTC-ExP	Model 3 E-OE-PTS-ExP	Model 4 E-OE-PTN-ExP	Model 5 E-OE-PTPV-ExP
$\mu_{\text{cyto}} =$ 0.001 Pa-sec	E: 7.5E-10* P: 8.8E-10* \dot{W} : 1.6E-9*	E: 9.7E-9* P: 4.0E-6* \dot{W} : 1.5E-7*	E: 2.0E-9* P: 1.2E-7* \dot{W} : 7.1E-9*	E: 2.4E-8* P: 9.9E-6* \dot{W} : 2.8E-7*	E: 3.0E-8* P: 1.9E-4* \dot{W} : 6.8E-7*
$\mu_{\text{cyto}} =$ 0.05 Pa-sec	E: 1.4E-9* P: 1.1E-7* \dot{W} : 3.8E-9*	E: 0.528 P: 0.449 \dot{W} : 0.488	E: 2.3E-3* P: 0.194 \dot{W} : 0.290	E: 0.497 P: 0.809 \dot{W} : 0.844	E: 0.500 P: 0.454 \dot{W} : 0.840
$\mu_{\text{cyto}} =$ 0.8 Pa-sec	E: 9.6E-8* P: 0.201 \dot{W} : 3.7E-6*	E: 0.352 P: 0.456 \dot{W} : 0.787	E: 0.044* P: 0.066 \dot{W} : 0.128	E: 0.224 P: 0.836 \dot{W} : 0.914	E: 0.279 P: 0.477 \dot{W} : 0.914
$\mu_{\text{cyto}} =$ 10 Pa-sec	E: 0.134 P: 0.695 \dot{W} : 0.399	E: 0.336 P: 0.453 \dot{W} : 0.776	E: 0.024* P: 0.064 \dot{W} : 0.069	E: 0.205 P: 0.824 \dot{W} : 0.918	E: 0.273 P: 0.476 \dot{W} : 0.909

†: We used Kruskal-Wallis test for all the statistical testings.

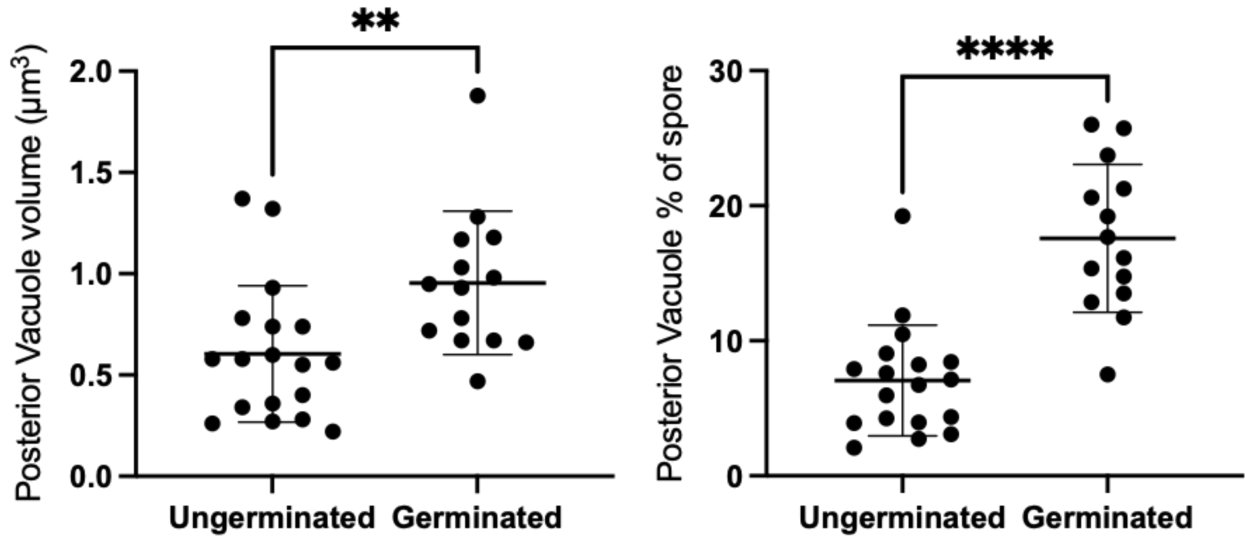







Figure S1: Volume of posterior vacuole in ungerminated and germinated spores. The volume of the vacuole was measured from SBF-SEM 3D reconstructions and is shown both as absolute measurements (left) and as a percentage of total spore volume (right). Posterior vacuoles in germinated spores, (mean = $0.955 \mu\text{m}^3$, std = $0.355 \mu\text{m}^3$, n = 14) are significantly larger in volume than posterior vacuoles in ungerminated spores (mean = $0.604 \mu\text{m}^3$, std = $0.337 \mu\text{m}^3$, n = 18) (independent t-test, $p = 0.0260$). Similarly, the volume fraction of posterior vacuole to the spore volume in germinated spores (mean = 17.58%, std = 5.48%, n = 14) is also significantly larger than the volume fraction in ungerminated spores (mean = 7.062%, std = 4.107%, n = 18) (independent t-test, $p < 0.0001$).

Pressure Requirement Formula of the 5 Hypotheses						
Hypotheses		Model 1	Model 2	Model 3	Model 4	Model 5
						
External Drag	along the tube	$\mathcal{D}_p(v, Lf(\epsilon))$				
	at the tip		$\mathcal{D}_p(v, R)$	$\mathcal{D}_p(v, R)$	$\mathcal{D}_p(v, R)$	$\mathcal{D}_p(v, R)$
Lubrication	two outermost layers of PT	$\mathcal{L}_p(v, h_{\text{sheath}}, L_{\text{sheath}})$	$\mathcal{L}_p(2v, h_{\text{sheath}}, L_{\text{sheath}})$	$\mathcal{L}_p(2v, h_{\text{sheath}}, L_{\text{sheath}})$	$\mathcal{L}_p(2v, h_{\text{sheath}}, L_{\text{sheath}})$	$\mathcal{L}_p(2v, h_{\text{sheath}}, L_{\text{sheath}})$
	uneverted & everted tube		$\mathcal{L}_p(2v, h_{\text{slip}}, L_{\text{slip}})$	$\mathcal{L}_p(2v, h_{\text{slip}}, L_{\text{slip}})$	$\mathcal{L}_p(2v, h_{\text{slip}}, L_{\text{slip}})$	$\mathcal{L}_p(2v, h_{\text{slip}}, L_{\text{slip}})$
	sporoplasm & everted tube					$\mathcal{L}_p(2v, h_{\text{slip}}, L_{\text{open}})$
Cytoplasmic Flow	cytoplasm in polar tube	$\mathcal{C}_p(v, L + L_{\text{sheath}})$	$\mathcal{C}_p(2v, L_{\text{open}})$		$\mathcal{C}_p(2v, L_{\text{open}})$	$\mathcal{C}_p(2v, L_{\text{open}})$
	polar tube content				$\mathcal{C}_p(2v, L_{\text{slip}} + L_{\text{sheath}})$	$\mathcal{C}_p(2v, L_{\text{slip}} + L_{\text{sheath}})$

Total Pressure Requirement		
All Hypotheses $\mathcal{D}_p(v, \ell) = 2\mu_{\text{surr}}v\ell/R^2$ $\mathcal{L}_p(v, h, L) = 2\mu_{\text{cyto}}\frac{v}{h + 2\delta}\frac{L}{R}$ $\mathcal{C}_p(v, L) = 2\mu_{\text{cyto}}L\sqrt{\frac{1}{2}(R + \delta)^2 - \frac{1}{4}R^2}$ $D = 100\text{nm}; R = 50\text{nm}$ $h_{\text{sheath}} = 25\text{nm}$ $h_{\text{slip}} = 6\text{nm}$	J-NOE-PTS-ExP $L_{\text{sheath}} = \frac{1}{2}(L_{\text{tot}} - L(t))$ $f(\epsilon) = \epsilon + 0.80685\epsilon^2 + 0.82854\epsilon^3$ $\epsilon = 1/\ln(2L/D)$	All Eversion Hypotheses $L_{\text{slip}} = \min(L(t), L_{\text{tot}} - L(t))$ $L_{\text{open}} = (2L(t) - L_{\text{tot}})H(2L(t) - L_{\text{tot}})$ $L_{\text{sheath}} = (L_{\text{tot}} - 2L(t))H(L_{\text{tot}} - 2L(t))$ $L_{\text{open}}(t_1) = 0$ $L_{\text{sheath}}(t_2) = 0$

Figure S2: Calculations for the pressure requirement of the polar tube (PT) firing process. Calculations were made by considering the contribution from external drag, lubrication between various structures, and cytoplasmic flow. Detailed breakdown of contributions for the five hypotheses listed in Figure 2 are shown, and the formula used for calculating different segment lengths based on observed PT length for each hypothesis is listed in the bottom. Symbols: μ_{cyto} : cytoplasmic viscosity; μ_{surr} : viscosity of the surrounding media; v : PT tip velocity; L : PT length; L_{tot} : total length of ejected PT; L_{sheath} : overlapping length of the two outermost layers of PT; L_{slip} : overlapping length of everted and uneverted PT; L_{open} : length of the PT that does not contain uneverted PT material; D : PT diameter; R : PT radius; ϵ : shape factor in slender body theory, defined as $1/\ln(2L/D)$; δ : slip length; h_{sheath} : lubrication thickness between the two outermost layers of PT; h_{slip} : lubrication thickness between everted and uneverted tube, or the cargo and everted tube.

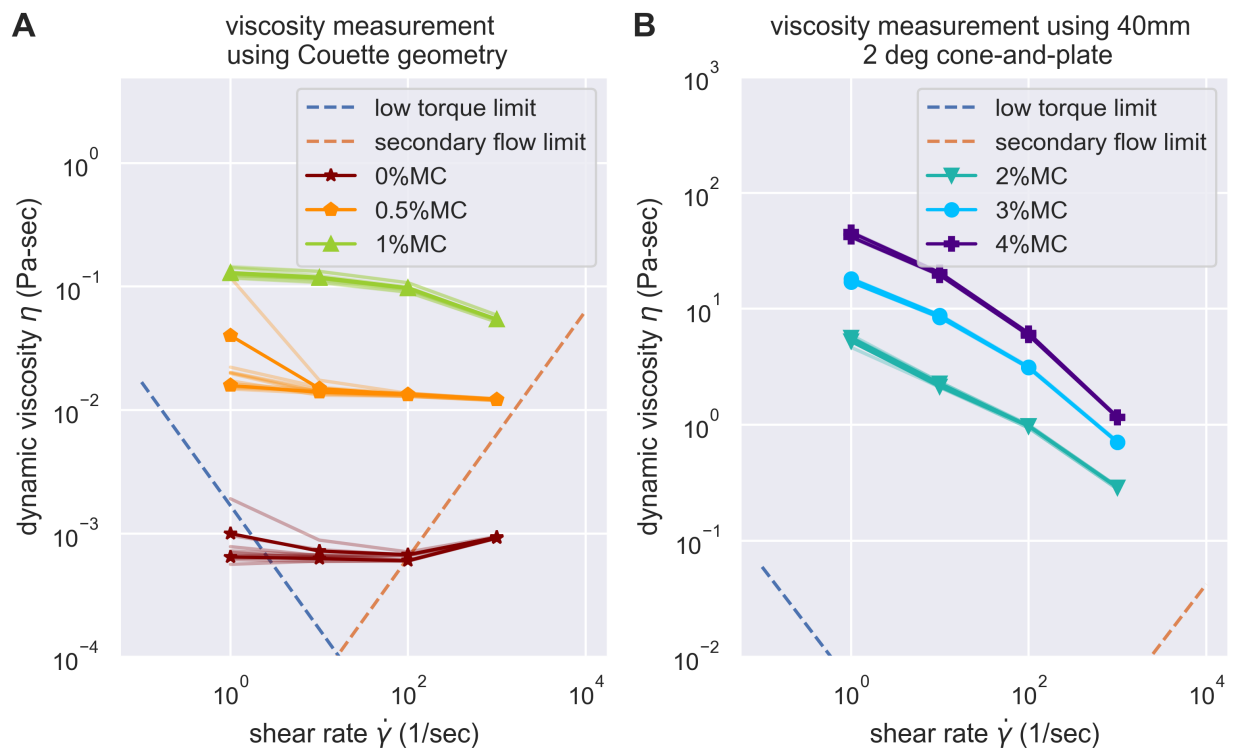


Figure S3: Evaluation of the experimental challenges of shear rheology in the measurement of buffer viscosity. Low torque limit and secondary flow limit was considered, according to the suggestion of Ewoldt et al.⁷ The data acquired were all above the experimental limit of shear rheometer, except for the buffer with 0% methylcellulose at the highest and lowest shear rate. However, as buffer with 0% methylcellulose is expected to be Newtonian, we can easily substitute it with measurements on other shear rate.

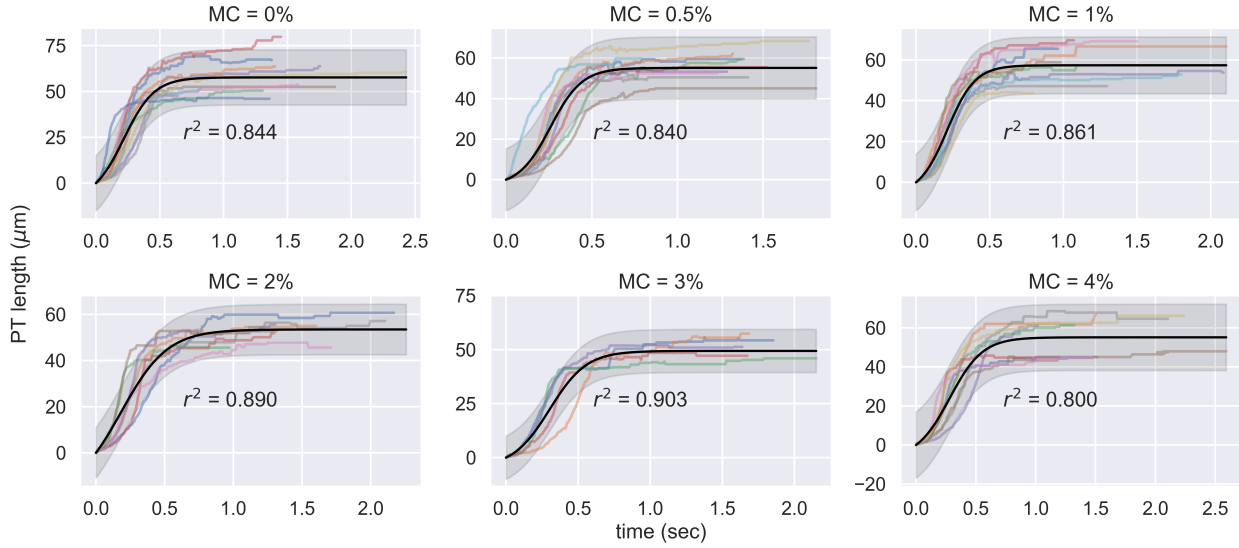


Figure S4: Experimental measurement of PT ejection kinematics of *A. algerae* spores in different concentrations of methylcellulose. The kinematics was fit to a sigmoid function $y = L(\frac{1}{1+e^{-k(x-x_0)}} - \frac{1}{1+e^{kx_0}})$. The additional term in the sigmoid function is to ensure the curve passes the origin. (0%: n=12; 0.5%: n=10; 1%: n=10; 2%: n=8; 3%: n=5; 4%: n=9)

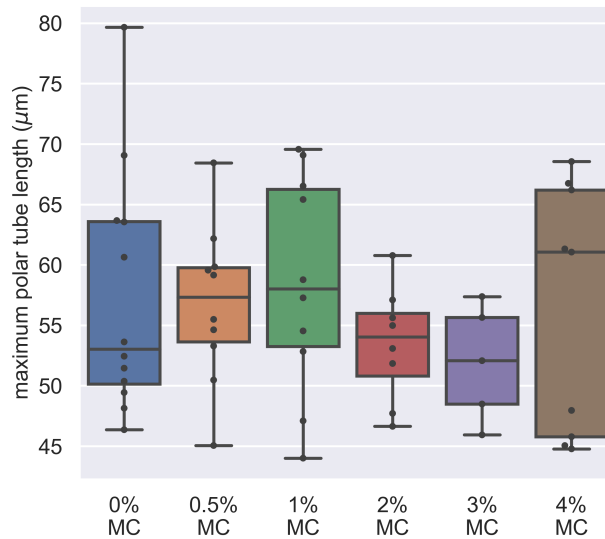


Figure S5: Dependence of maximum PT length on the methylcellulose concentration in germination buffer. The x-axis shows the different concentration of methylcellulose we used for our experiments, and the y-axis shows the maximum PT length of each germination event. The maximum PT length does not depend on the concentration of methylcellulose in the germination buffer. ($p = 0.743$, Kruskal-Wallis test)

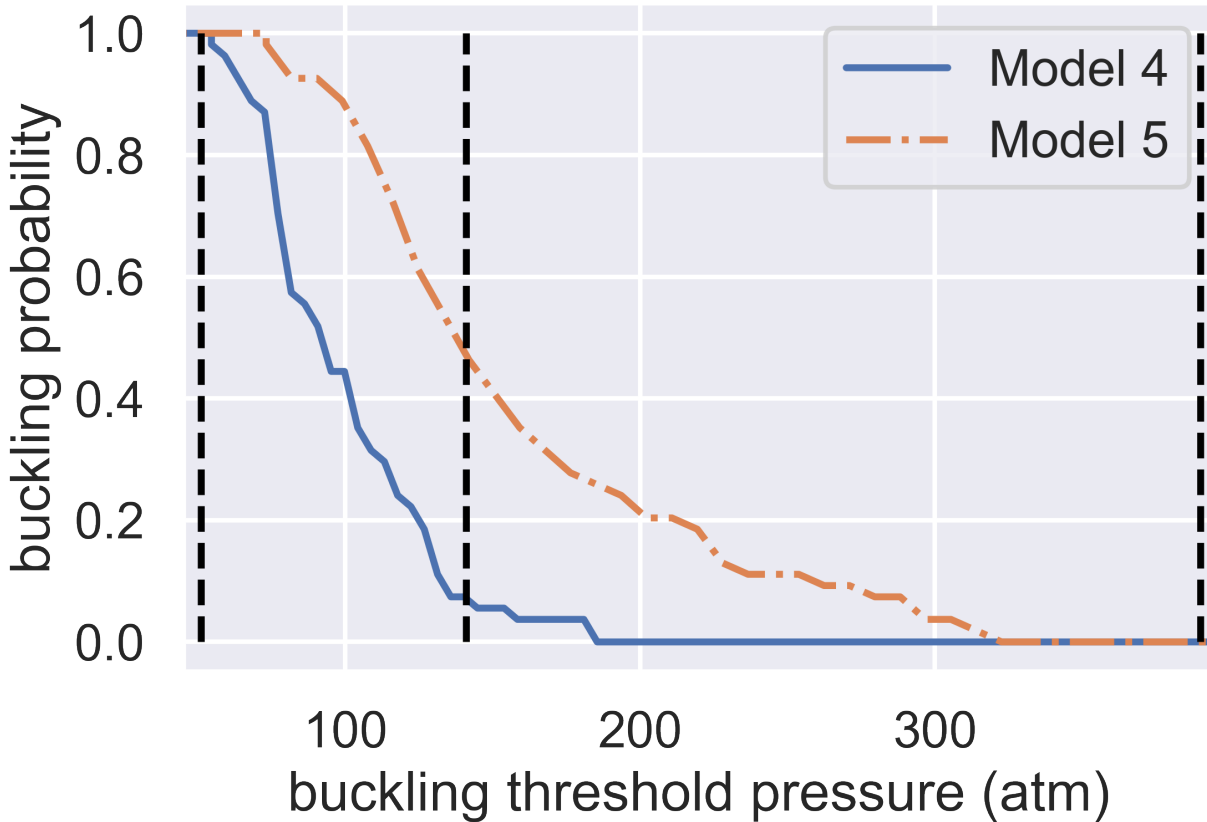


Figure S6: Dependence of spore buckling probability on the threshold pressure of spore wall buckling. The x-axis shows the buckling threshold we choose while the y-axis shows the predicted probability of buckling. The 2 curves are predictions from Model 4 and Model 5. The 3 vertical dashed lines show the minimum (51 atm), geometric averaged (141 atm), and maximum (390 atm) predicted buckling threshold.

References

- (1) Ohshima, K. A preliminary note on the structure of the polar filament of *Nosema bombycis* and its functional significance. *Annotationes zoologicae Japonenses* **1927**, *11*, 235–243.
- (2) Weiser, J. Klíč k určování Mikrosporidií. *Acta Societatis Scientiarum Naturalium Moraviae* **1947**, *18*, 1–64.
- (3) Dissanaïke, A. S.; Canning, E. U. The mode of emergence of the sporoplasm in Microsporidia and its relation to the structure of the spore*. *Parasitology* **1957**, *47*, 92–99.
- (4) Keeling, P. J.; Fast, N. M. Microsporidia: biology and evolution of highly reduced intracellular parasites. *Annual review of microbiology* **2002**, *56*, 93–116.
- (5) Findley, A. M.; Weidner, E. H.; Carman, K. R.; Xu, Z.; Godbar, J. S. Role of the posterior vacuole in *Spraguea lophii* (Microsporidia) spore hatching. *Folia Parasitologica* **2005**, *52*, 111–117.
- (6) Lom, J.; Vavra, J. The mode of sporoplasm extrusion in microsporidian spores. *Acta Protozoologica* **1963**, *1-13*.
- (7) Ewoldt, R. H.; Johnston, M. T.; Caretta, L. M. In *Complex Fluids in Biological Systems*; Spagnolie, S. E., Ed.; Springer, New York, NY, 2015; pp 207–241.